Progress in Chemical and Biochemical Research

Journal homepage: www.pcbiochemres.com

Original Research Article

PVDF/ MWCNT hollow fiber mixed matrix membranes for gas absorption by Al_2O_3 nanofluid

Adel Talavari[1], Bijan Ghanavati[1,*], Alireza Azimi[1], Soheil Sayyahi[2]

[1]*Department of Chemical engineering, Mahshahr Branch, Islamic Azad University, Mahshahr, Iran*
[2] *Department of Chemistry, Mahshahr Branch, Islamic Azad University, Mahshahr, Iran*

ARTICLE INFO

Article history

Submitted: 2021-01-24
Revised: 2021-02-16
Accepted: 2021-02-24
Available online: 2021-03-30
Manuscript ID: PCBR-2101-1177
DOI: 10.22034/pcbr.2021.270178.1177

KEYWORDS

Mixed Matrix Membranes,
AL_2O_3,
Nano Fluid,
MWCNT,
Hydrophobicity.

ABSTRACT

The study aims to investigate mixed matrix membranes for absorption of CO_2in gas-liquid contacting process by AL_2O_3 nanofluid as liquid absorbent. PVDF/MWCNT hollow fiber mixed matrix membranes were fabricated absorbent and characterized via relevant characterizations. This study showed that the addition of MWCNT to the matrix led macro cavities to be expanded at the cross section of the membrane. According to the results of gas permeation, surface porosity experienced an increasing trend and in contrast surface pore size reduced. By placing the CNTs in porous PVDF, an increase in the surface contact angle and hydrophobicity of the composite membranes was revealed which could be related to the hydrophobic nature of the added nanopaticles as well as increasing the absorbent average surface roughness.

Highlights

- This study showed that the addition of MWCNT to the matrix led macro cavities to be expanded at the cross section of the membrane.
- Surface porosity experienced an increasing trend and in contrast surface pore size reduced.
- By placing the CNTs in porous PVDF, an increase in the surface contact angle and hydrophobicity of the composite membranes was revealed which could be related to the hydrophobic nature of the added nanoparticles as well as increasing the absorbent average surface roughness.

* Corresponding author: Ghanavati, Bijan
✉ E-mail: bijanghanavati@yahoo.com
☏ Tel number: 989163547899

GRAPHICAL ABSTRACT

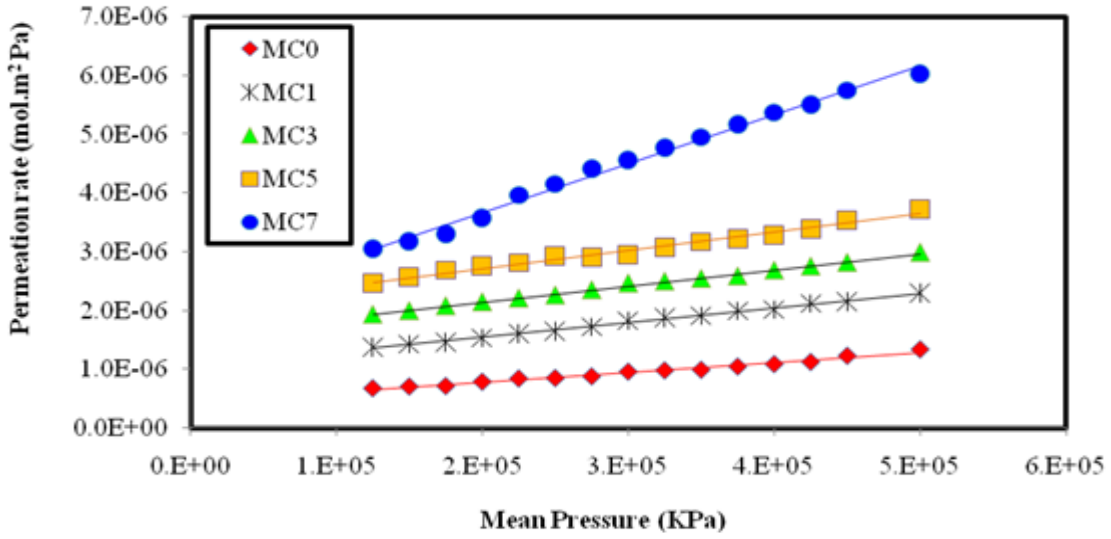

1. Introduction

In this research, there are two main parts. One of them is the synthesis of asymmetric hollow fiber membranes and improvement of membrane properties by depositing mineral nanoparticles to increase CO_2 uptake in gas-liquid contacting process. Another is to test the efficiency of the fabricated membranes using nano-fluid as absorbent and compare the results with other hand-made and commercial membranes in the literature [1]. The effects of inorganic nanoparticles in different amounts on the physical properties, structure and efficiency of the membrane were studied to find the optimal value. Increasing membrane permeability or decreasing mass transfer resistance was a challenge for the produced membranes, which can be achieved by increasing the effective porosity of the membrane, improving the structure and increasing the hydrophobicity of the membrane [2-4].In order to increase the porosity and hydrophobicity of the membranes, the synthesized MWCNT nanotubes with different loadings was incorporated into the polymeric matrix. Then, the physical absorption of CO_2 through aqueous Al_2O_3 nanofluid in the membrane contactor was investigated. This study was a preliminary experimental design for the fabrication of polymer membranes whose defects are eliminated as much as possible and used in the gas-liquid contactor. Polyvinylidene fluoride (PVDF) polymer was selected as a continuous fabric for making hollow fiber membranes by phase inversion method. PVDF is a rubbery polymer having viscoelastic behavior and periodicity of CH_2 and CF_2. This partially crystalline polymer has good chemical resistance against all weak bases, salts and strong acids, and also high hydrophobicity, mechanical strength and hardness [5].

The removal of CO_2 from gas pipelines by membrane contactors has been of interest to researchers since the 1980s. Qi and Kassler [6] were the first to introduce porous membrane contactors for use in CO_2 removal, and then did a lot of research to expand their idea. Many researchers then considered various parameters such as absorbent type, membrane type, module type and operating conditions to increase the efficiency of the membrane system in CO_2 removal. Basic requirements of the membranes applied in gas-liquid contacting processes are high porosity to reduce mass transfer resistance and high hydrophobicity to prevent liquid penetration into the gas-filled pores on the membrane surface. Mansoorizadeh and Fauzi

Ismail [7] improved the structure of fabricated poly vinylidene fluoride (PVDF) membranes to increase CO_2 uptake by adding insoluble additives in the polymer solution. Atcharyavat et al. [8] fabricated PVDF membranes by phase inversion method for CO_2absorption and showed that the asymmetric membrane structures are more suitable for use in gas-liquid contactors compared to symmetric membranes. The applications, advantages, and disadvantages of gas-liquid membrane contactors were further explored by Qiand Kassler [9-11], Gobelmann & Huang [12] and Dimontigeni [13-15]. Li and Chen [16] also investigated the effect of chemical absorbents on CO_2 uptake in hollow fiber membrane contactors.

2. Experimental

2.1 Materials

Wet-phase inversion technique was the method of fabricating hollow fiber membranes. The experimental set-up and procedure details can be found elsewhere [17]. Table 1 showsthe composition of the prepared spinning solutions and as well as the membrane spinning conditions and the membranes are coded based on their nanofiller loading. the solution viscosity of the provided solutios also was measured since.

Table 1. Composition of polymeric spinning dopes and the membrane spinning conditions.

Solution Codes	PVDF wt.%	NMP wt.%	LiCl wt.%	CNT (percentages of polymer)	Membrane spinning parameters	
MC0	18	79.5	2.5	0	Dope extrusion rate (mL/min)	4.5
MC1	18	79.5	2.5	1	Bore flow rate (mL/min)	1.7
MC3	18	79.5	2.5	3	External coagulant	Tap water
MC5	18	79.5	2.5	5	Bore composition (wt%)	Water/NMP; 20/80
MC7	18	79.5	2.5	7	Spinneret o.d./i.d. (mm)	1.2/0.55

PVDF is soluble in the most common solvents however NMP was used as a non-volatile solvent due to its strong interaction with PVDF, good chemical stability, high boiling point (204.3 °C) and good dispersion of mineral nanoparticles in this solvent.1-Methyl-2-pyrrolidone (> 99.5% NMP>) was purchased by MERCK company and used as a polymer solvent without any pretreatment.

Pore-forming additives

Membrane properties are often modified by adding small amounts of molecular insoluble additives to the polymer solution. In this work, the mineral salt of lithium chloride (99.5% LiCl, Sigma-Aldrich) was added to the polymeric since it has high solubility in water (832 g/l) and hence can be easily dissolved by water and remove from the membrane fabrication stage.

Inorganic Fillers

Extra strength, light weight and nanoscale dimensions make MWCNTs conductive in the group of conductive and semiconductor materials. Due to the special properties of neural tissues, the use of nanoscale compounds is more appropriate than other materials. Due to their special shape, this substance can selectively pass through the body's biological barriers. In addition, its characteristics and dimensions are similar to many structural elements of the MWCNT of nervous systems (ion channels, protein signaling, and elements of the neural skeleton). This feature can be considered as an

advantage in increasing molecular level interactions and thus better control of physiological activities and neuronal information processing.

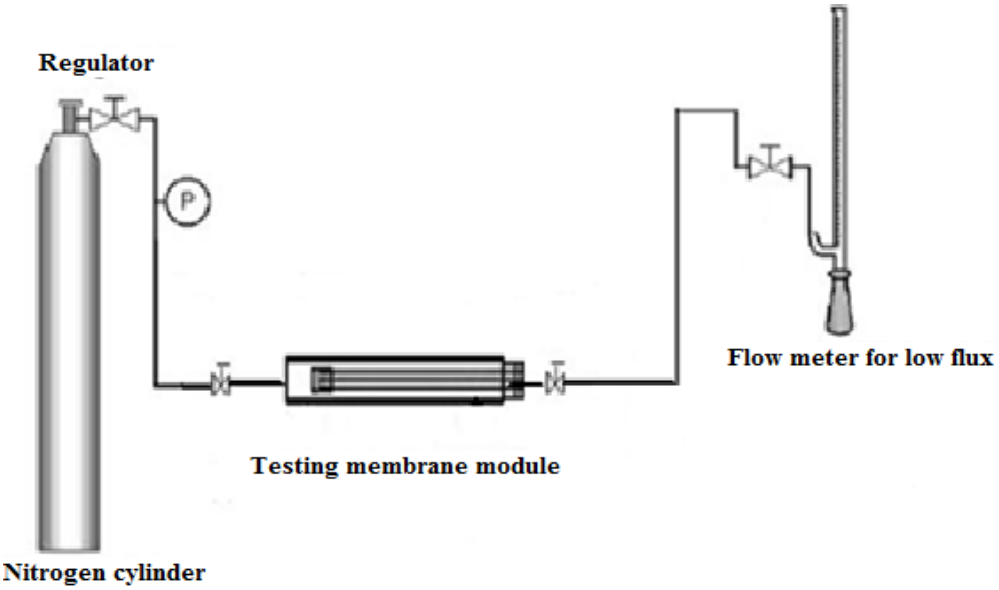

.

Figure 1. Making porous hollow fiber membranes

Preparation of spinning solution

Hollow fiber membranes were prepared by a combination of wet phase inversion and solution dispersion methods. Details of the laboratory setup and production method are described elsewhere [17]. The synthesized filler, polymer and LiCl pellets were dried in oven at 60 ° C for 72 hours to remove air humidity. In this study, nanotubes with different weight ratios to the base polymer were added to the solution. Therefore, a base solution with the following concentrations was selected. In order to prepare polymer solutions, first different amounts of MWCNT were added to the base solution as described, in which the weight of MWCNT per 100 g of the base solution with selection codes is provided for each membrane based on the amounts of nanoparticles in solution. MWCNT fillers were initially dispersed in solvent (NMP) and dispersed in an ultrasonic shaker for 60 minutes at 40 ° C to prevent agglomeration. LiCl was then added for at high stirring by a stirrer at 60 ˚C, and then the polymer pellets were gradually added to the mixture and kept stirring overnight to ensure complete dissolution of the polymer and complete mixing of the filler. The solutions were eventually degassed using ultrasonication and kept at room temperature for 5 hours. It should be noted that the composition of the prepared solutions was based on articles. The viscosity of polymer solutions as a factor affecting the membrane structure was measured by a viscometer.

How to prepare Nanofluid?

The nanofluid was prepared by dispersing predetermined amounts of nanoparticles in purified water as the base absorbent. Nanofluid based on water containing 0.1 wt% of Al_2O_3absorbentabsorption was prepared based on the results reported in the articles [18]. To prepare, 1 g of Al_2O_3 powder was gradually dispersed in DI with a stirrer under intense stirring after drying in a furnace for 2 h at 65 °C.

Stirring of the solution containing the suspended particles was continued until the absorption test to prevent clumping and deposition of the suspended nanotubes.

Measurement of contact angle and liquid entry pressure of water (LEPw)

Although the numerous advantages of membrane based absorption process over conventional absorption devices have been demonstrated, recent advances in this field are still on a laboratory scale and the stability of membrane performance in the long run has rarely been absorption studied. Wetting and morphological changes of the membrane used in membrane contactors mainly by membrane materials (contact angle, roughness, etc.), properties of the fabric made (pore size, porosity and morphology) and operating conditions assuming suitability the selected absorbents are affected [22].The sessile drop method using a goniometer (model G1, Krüss GmbH, Hamburg, Germany) was used to measure the surface contact angle of the membranes. The water droplet was placed by a syringe on the sample surface and the change in the image was monitored by a high resolution camera. Liquid entry pressure of water (LEPw) is the pressure that must be applied onto water absorbent before penetrating into dried membrane pores. It depends on the size of the largest membrane surface pore and the membrane surface hydrophobicity [36]. Distilled water was sent to the inside of the hollow fibers and then the pressure was slowly increased at 0.5 bar interval and kept constant for at least 10 min at each pressure. Whenever the first water droplets appeared on the outer side of the hollow fiber membranes, the pressure was recorded as the value of LEPw for each membrane.

Mass transfer measurement

In the separation of gases by non-porous polymer membranes and liquid membranes, the solubility-diffusion mechanism is dominant. Separation in processes such as reverse osmosis, diffusion-evaporation and separation of gases by dense membranes whose polymer chain gap space is less than 5% in this mechanism are classified [24]. This size is in the range of motion and vibration of molecular objects, and empty spaces are not in a fixed place. According to this mechanism, the particles first penetrate to the membrane from the boundary layer formed on the surface of the membrane, then absorption takes place and after penetration, from the other side the membranes are detached. A noteworthy point in this model is that the separation operation takes place for two reasons, namely the difference in solubility and the difference in permeability [25]. Therefore, components that are approximately the same size but have different solubility can be separated by these membranes. The industry usually uses heterogeneous membranes to increase the mass transfer flux, which consists of a very thin, dense layer on the porous layer. The porous layer is mostly used to increase the location of the membrane [26]. In articles, the solubility-diffusion mechanism is mostly the mass transfer mechanism in dense and non-porous membranes. The total mass transfer coefficient (KOL) is determined by Equation (1).

$$K_{OL} = \frac{Q_L (C_L^{out} - C_L^{in})}{A \Delta C_L^{Av}} \qquad (1)$$

In Equation (1), the parameter KOL is the total mass transfer coefficient (m.s-1), QL is the liquid flow rate (m^3.s-1), CL is the concentration of dissolved gas (CO_2) in the liquid (mol.m^{-3}), A is the contact range (m^2) based on the internal diameter of the hollow fiber membrane and the mean difference of the logarithmic concentration between the dissolved gas membrane by Equation (2).

$$\Delta C_L^{Av} = \frac{(HC_g^{in} - C_L^{in}) - (HC_g^{out} - C_L^{out})}{Ln((HC_g^{in} - C_L^{in}) / (HC_g^{out} - C_L^{out}))} \qquad (2)$$

The average absorption flux calculated with a

simple mass balance of CO_2 concentration along the hollow fibers using Equation (3).

$$J_{av} = \frac{Q_L m C_g (1 - \exp(-K_{OL} \pi d_i l / Q_L))}{\pi d_i L} \quad (3)$$

Since the absorption flux is L, the effective length of the hollow fibers (m). Also the resistance of the series model, the total resistance is a combination of the resistors mentioned above, which are calculated from Equation (4) [27-29].

$$\frac{1}{K_{OL}} = \frac{1}{K_L} + \frac{Hd_i}{K_m d_{lm}} + \frac{Hd_i}{K_g d_o} \quad (4)$$

The total mass transfer coefficients based on the liquid phase ($m.s^{-1}$), kL, km, kg, are the independent liquid phase mass transfer coefficients. H represents the artistic constant for water at 25 °C is 0.831 [30]. d_i, do, d_{lm} are the average inner, outer and logarithmic diameters of the membrane, respectively, which can be calculated by ignoring the gas phase resistance of the liquid mass transfer coefficient in the liquid flow mode inside the hollow fibers using Equation (5).

$$Sh_L = \frac{K_L d}{D_A} = \sqrt[3]{3.67^3 + 1.62^3 Gz} \quad (5)$$

where the Sherwood number, Gz is the Gertz number, D is the fluid permeability coefficient, L is the length of the hollow fibers and V is the velocity of the liquid, which is approximately proposed by Kumar et al. In order to further evaluate the industrial efficiency of hollow fiber membranes, the stability of CO_2absorption performance of membranes over a long period of about 200 hours was investigated.

Evaluation of the efficiency of membranes made for the absorption of carbon dioxide

CO_2absorption test using pure CO_2 as a soluble gas and one of two water-absorbing fluids or water-suspended Al_2O_3 nanoparticles to evaluate the performance of composite membranes as well as the potential of nanofluids prepared for CO_2absorption and Membrane mass transfer resistance measurement was performed. To prepare a membrane contactor module for the absorption process, ten piece of hollow fiber membranes with the effective length of 17.5 cm were placed in a stainless steel tube.

Pure CO_2 was sent to the shell side of the module (1 bar_g) while the absorbent at a pressure of 1.2 barg was sent to the inside of the hollow fibers. The concentration of CO_2absorbed in the effluent was measured by titration method using 0.02 M sodium hydroxide solution (NaOH) and phenolphthalein solution as an indicator. Then the total CO_2absorption flux was calculated using the fluid flow rate and CO_2 concentration at the output of the module and was reported as mol CO_2/ m^2.s.

3. Results

Physical and structural properties of synthesized MWCNTs

To confirm successful formation of the MWCNTs' nanotubes, low and high magnification TEM images were shown in Fig. 2.

As can be seen, a layer of disordered amorphous carbon have wrapped MWCNTs (Fig. 2 (a))which should be considered as intrinsic surface chemistry of the synthesized nanotubes due to using CCVD method as synthesizing method of MWCNT [38]. The higher magnification TEM image (Fig. 3(b)) is higher magnification TEM image that shows a thick layer encapsulated at the CNT tips which most likely are amorphous carbon and metal particles.

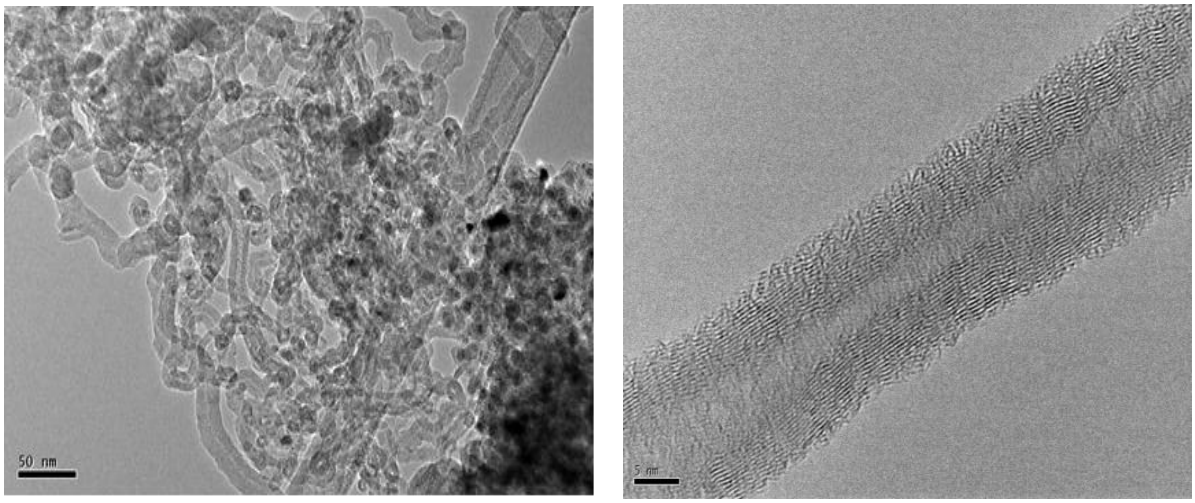

(a) (b)

Figure 2. TEM images of the producednanotubes

FESEM micrographs of the synthesized nanotubes are shown in fig. 3. It can be seen that MWCNTs are highly interwoven and have large diameter dispersion due to the placement of irregularly spaced carbon with different thicknesses on the surface and side walls of the nanotubes. The surface compositions of the synthesized MWCNTs using EDX revealed the main constituents of the surface are Carbon (C), oxygen (O), iron (Fe), cobalt (Co) and aluminum (Al) with the percentages of 68.1, 13.3, 1.2 and 2.9, respectively.

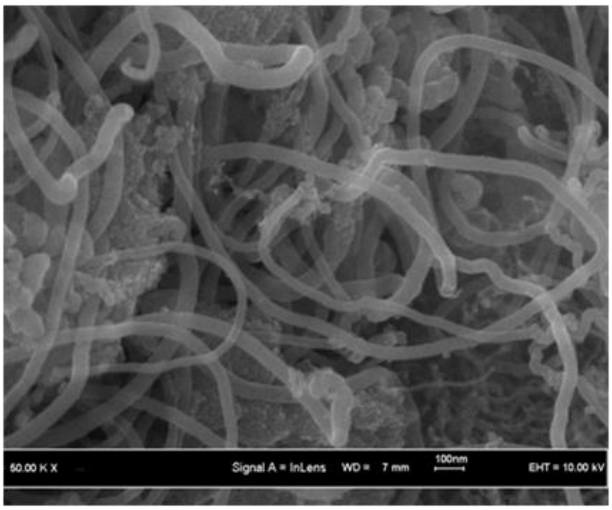

Figure 3. FESEM image of synthesized nanotubes

Since the main component was carbon that is hydrophobic in nature, an improved surface hydrophobicity for the fabricated composite membranes can be predicted.

FTIR spectra of the synthesized MWCNTs shown in fig. 4 revealed significant bands in the range of 3500-3000 cm-1which most likely is related to the hydroxyl groups formed by the absorption of water moisture on the surface of the nanotubes. The absorption of moisture can be ascribed to the irregular wall of MWCNTs as well as the presence of defects on the surface and along the margins of the nanotubes [32]. Therefore, the C-H elongation around 2900 cm^{-1} can be easily observed through FTIR. Poor absorption peak visible at 1360 cm^{-1} can also be attributed to C-O elongation. In addition, an absorption band around 2370 cm^{-1} can be attached to CO_2 molecules.

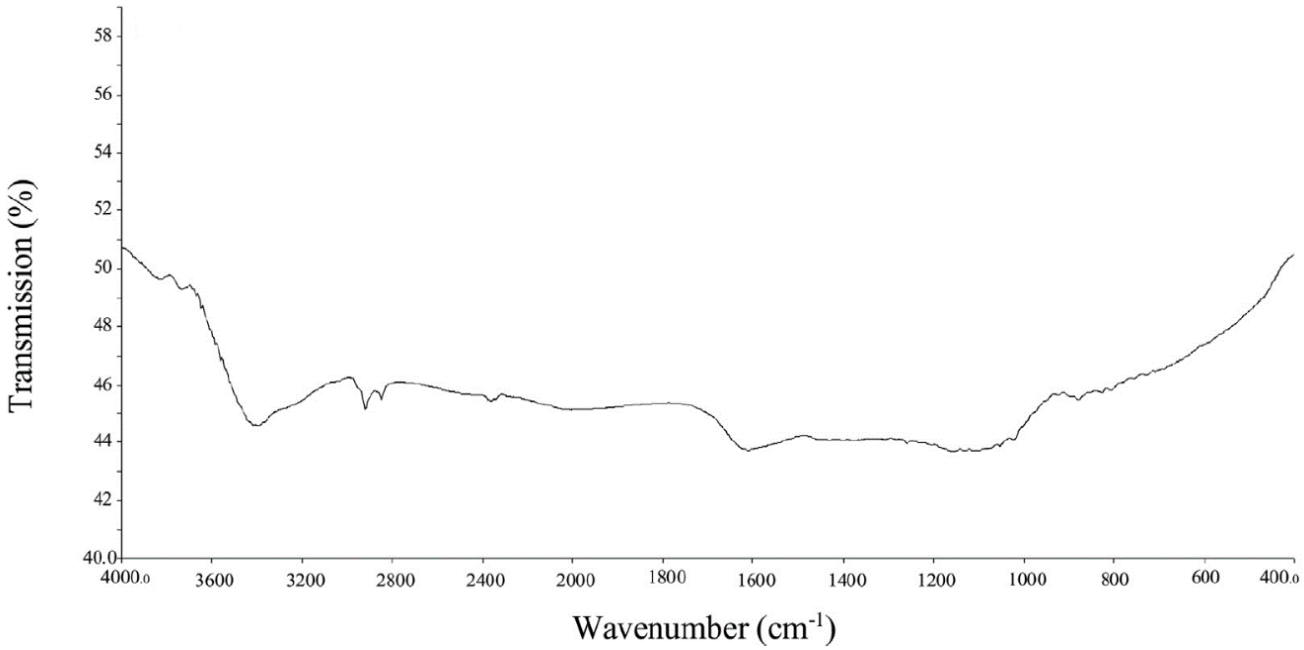

Figure 4: FTIR absorption spectrum of synthesized nanotubes

The FESEM images of the prepared membranes illustrated in fig. 5 show asymmetric structure for all the membranes consisting of a thin skin layer, finger-like pores, and sponge-like structures. It can be seen that the membrane with no filler added (Fig. 5(a1)) has less extension of the finger-like macrovoids, while the embedment of the MWCNT nanofiller into the membranes led finger-like structure to fully extend throughout the hollow fibers. This is most likely related to the rate of phase inversion as well as the rate of liquid-liquid phase separation which increase by loading of the nanotubes. Regarding the inner surface micrographs (Fig. 5(c1)(c2)), using 80% aqueous NMP bore fluid composition led phase inversion process to be delayed and hence inner skinless and open microporous structure in contrast to the outer surface (Fig. 5(a2)(b2)) was formed. An inner surface of the membranes with no skin can reduce the mass transfer resistance and improve the mass transfer rate.

The results of the gas permeation test are shown in fig. 5. The average pore size and effective surface porosity of the membranes were measured by using the slope and intercept of the lines passed through the experimental data. The results shown in Table 2indicates that the gas permeation increases gradually with loading of nanoparticles and MC_7 composite membrane with the highest amount of filler has the highest N_2 gas permeation rate. However, the steep slope of the MC_7 MMM confirms the size of the large pores on the outer shell of the membrane. The effective surface porosity also increased by loading up to 5 wt% and then reduced. In addition, the mean surface pore size in contrast to the trend of the surface porosity reduced for the prepared membranes up to 5 wt% loading and then drastically increased for the MC7 MMM.

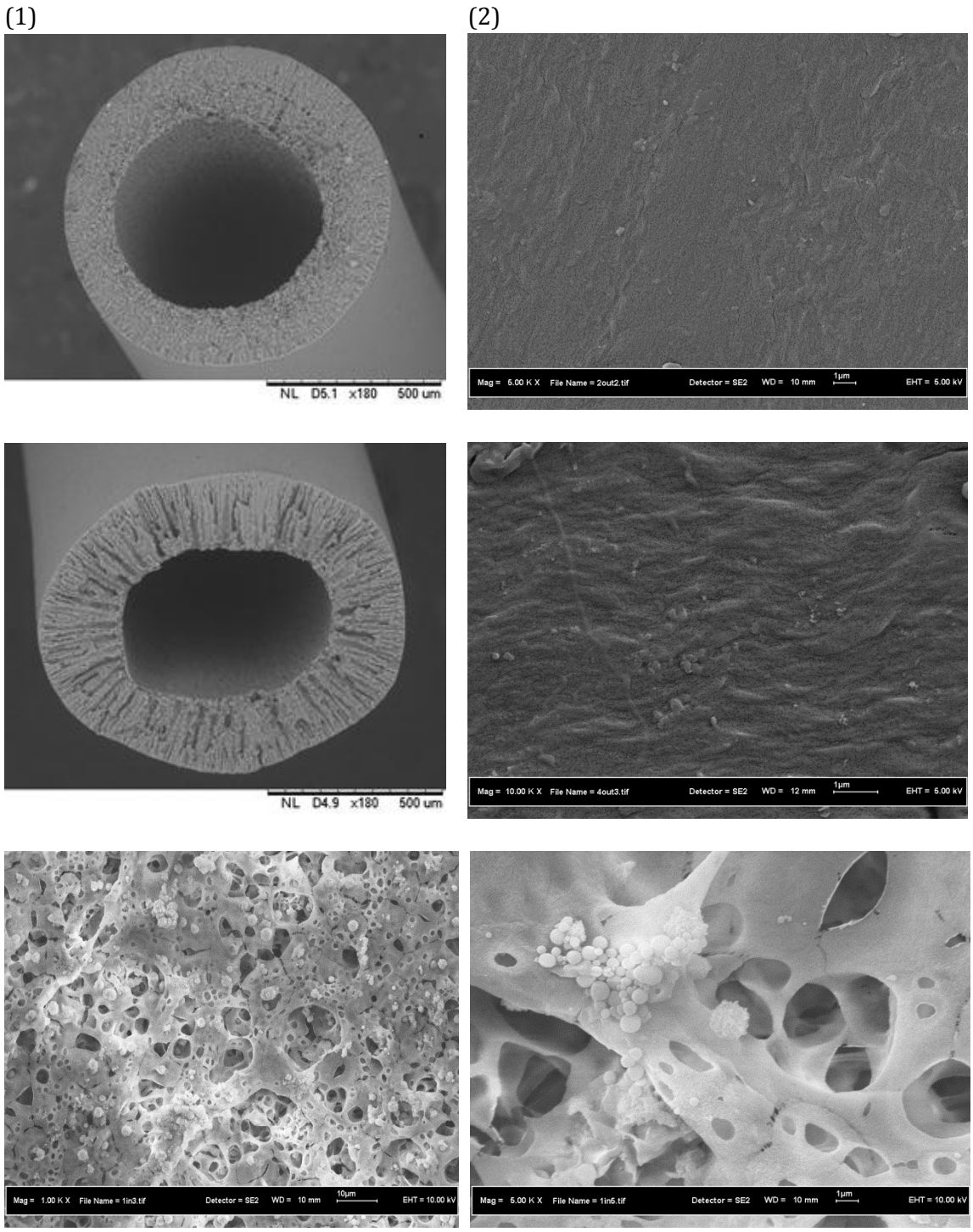

Figure 5: Hollow fiber membrane images; (a): MC0; (b): MC5; (1) SEM cross-sectional images; and (2) FESEM outer surface images; (c1, c2): FESEM inner surface images.

The measurement of the contact angle exhibited enhancement in the surface hydrophobicity of the fabricated membranes and the contact angle increased from 83° ± 1.5 for the MC0 to 103° ±1.5 for the MC5 and then reduced to 87 ± 1.0 for the MC7.

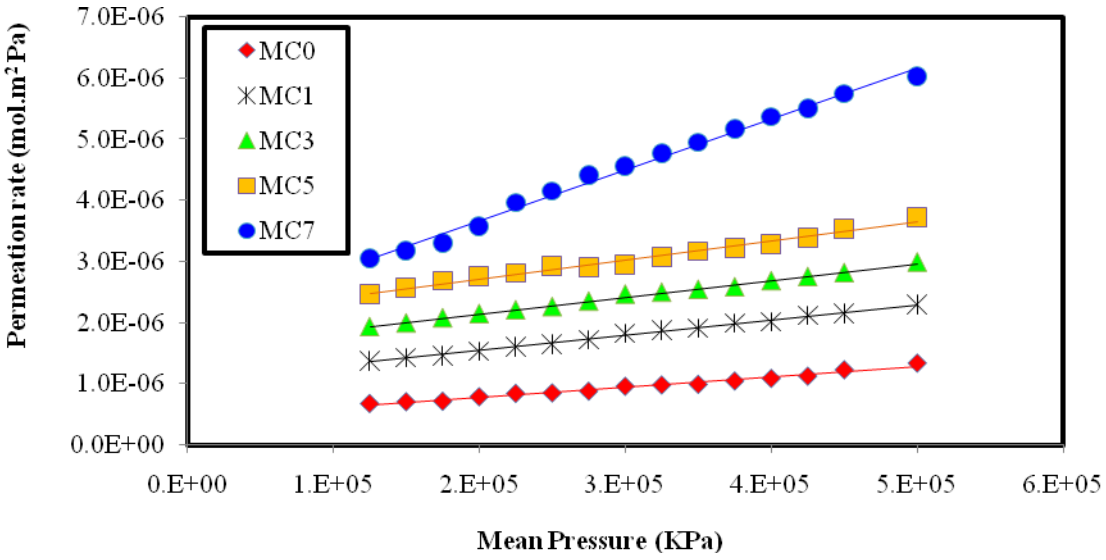

Figure 6. The rate of penetration of total gas against the pressure of the fabricated membranes

Table 3: Hollow fiber membrane characteristics.

Membrane	Dope solution viscosity (centipoise)	Permeance of N_2 gas at 7 bar_g (10^{-6}mol/m²spa)	Effective surfacepo rosity(m^{-1})	Mean pore size,$r_{P,m}$ (nm)	Contact angle (θ)	LEPw (bar)	Membrane Mass transfer resistance (10^3 $(m/s)^{-1}$)
MC0	1650	1.23	26	131.1	83° ± 1.5	6.5 ±0.5	1.17
MC1	1716	2.15	64	127.2	89°± 1.25	8.5±0.5	1.09
MC3	1744	2.8	136	91.2	96° ± 1.5	8.5 ±0.5	1.07
MC5	1756	3.53	209	78.3	103° ±1.5	10 ±0.5	0.68
MC7	1776	5.7	70	222.1	87 ± 1.0	5.5± 0.7	0.34

The higher surface hydrophobicity of the fabricated MMMs most likely was related to the highly hydrophobic nature of the incorporated MWCNTs used to modify the membrane surfaces. As a result of increasing contact angle as well as reducing the membrane surface pore size, the fabricated MMMs experienced significant enhancement in LEPw as a crucial factor for the membranes applied in contactor application (see Table 3).The LEPw of 6.5±0.5 bar for the MC0 was increased to 10 ± 0.5 bar for the MC5. Figure 6 and 7exhibitedthe CO_2absorption flux of membranes as a function of absorbent fluid velocity. As can be seen, the absorption flux increases by increasing fluid velocity. The flux of the membranes also progressively increases by loading of the nanofiller from MC0 to MC5 and then the flux slightly reduced for the MC7 MMM. The enhanced flux was most likely ascribed to the increased surface hydrophobicity and LEPw as well as he extended finger-like macrovoids. The flux of MC5 at a liquid velocity of 2.5 m/s was 3.85 × 10^{-3} mol/m² s was 200%, 79%, 42% and 74% higher than that of MC0, MC1, MC3 and

MC7 MMMs. Figure 7 also revealed the effect of the existence of the nanoparticles in the absorbent fluid on the membrane performance.

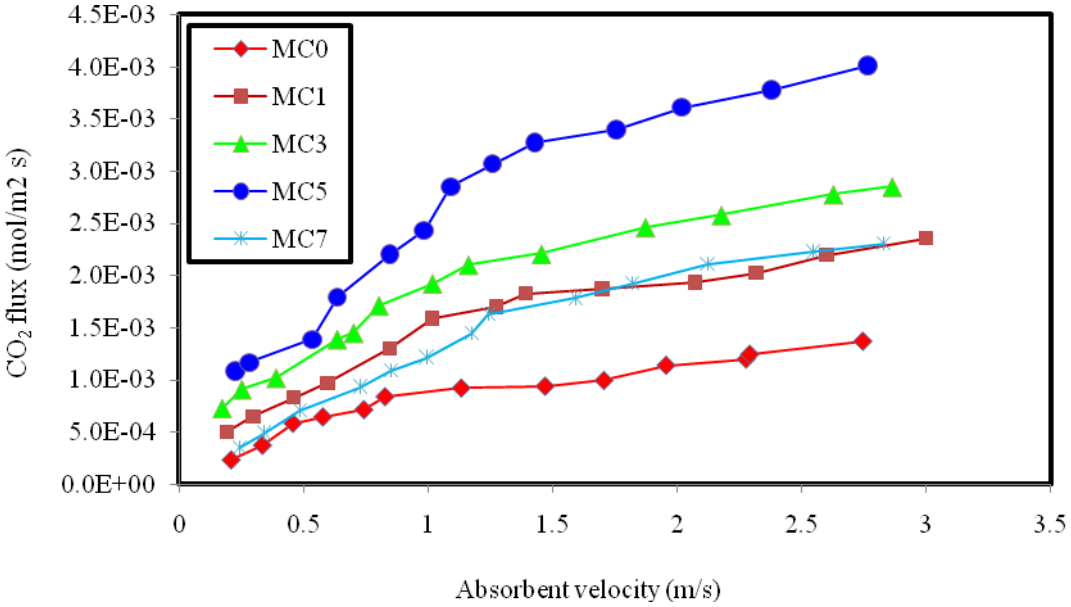

Figure 7. CO_2 absorption flux of membranes as a function of fluid velocity (pure CO_2 on the shell side, Qg = 150 ml / min, TT = 25 ºC, Pg = 105 1 1 Pa, Pl = 1.2 × 105 Pa nano-fluid on the inside Hollow fibers

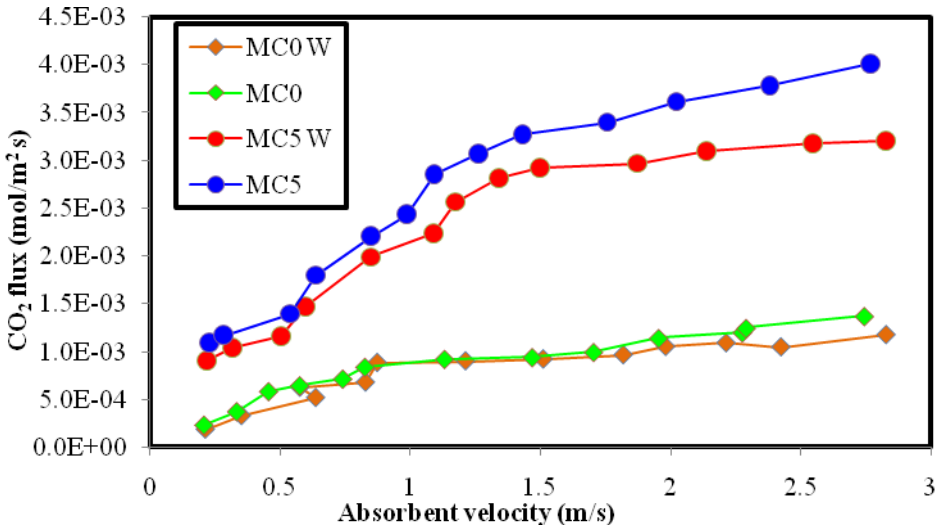

Figure 8. Membrane CO_2absorption flux as a function of absorbent fluid velocity (pure CO_2 on the shell side, Qg = 150 ml / min, TT = 25 ºC, Pg = 105 1 1 Pa, Pl = 1.2 × 105 Pa, nano-fluid and water to Absorbent title on the inside of your empty fibers

It can be seen from the figure that the flux enhancement is more pronounced where the absorbent liquid is changed from the pure water to the nanofluid. This is related to the increasing the turbulancy of the absorbent fluid as well as the shuttle effect. The overall mass transfer

resistance of the membranes also was measured by Wilson plot and exhibited in figure 8 where $1/K_O$ as a function of $V_l^{-0.93}$ is plotted. The results showed that the MC5 possesses the lowest mass transfer resistance. In addition, the results indicated that the mass transfer coefficient of the liquid enhances by increasing liquid velocity.

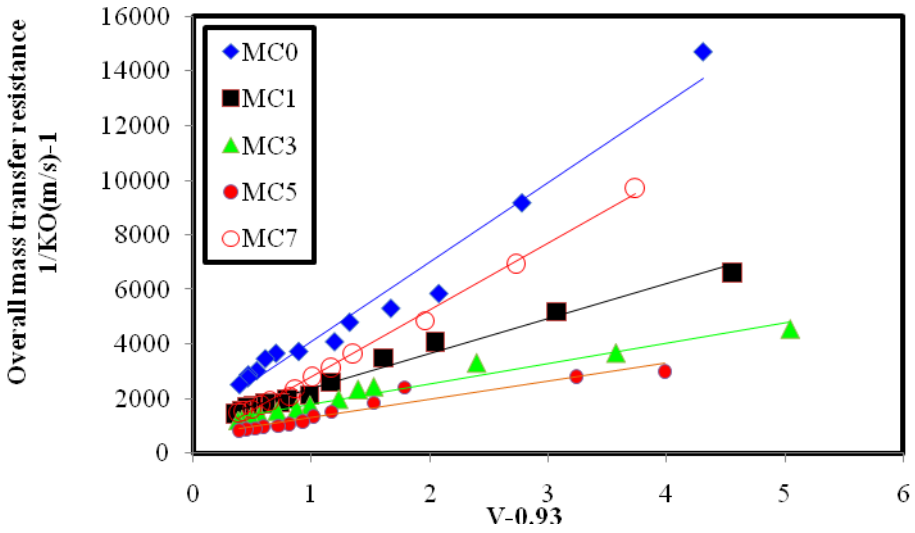

Figure 9. Wieslon made membranes (pure CO_2 and nano fluid as absorbent).

Figure 9 shows the prolonged absorption test of MC5 MMM as the best performing membrane among all the prepared membranes in short-term contactor test. The test was conducted over 200 hrs and the absorption flux was almost stable until the end of the experiment. Rezaei et al. [36] and Atchariaut et al. [37] observed similar to the results of this study, showed the stability of PVDF membrane absorption efficiency over a long period of time. However, Mavroudi et al. [38] reported a decrease in the absorption process efficiency for PVDF for PP membranes during the first 2-20 hours of operation using water as an absorbent [39]. They related the decrease of the efficiency to the gradual wetting of the membrane pores with time.

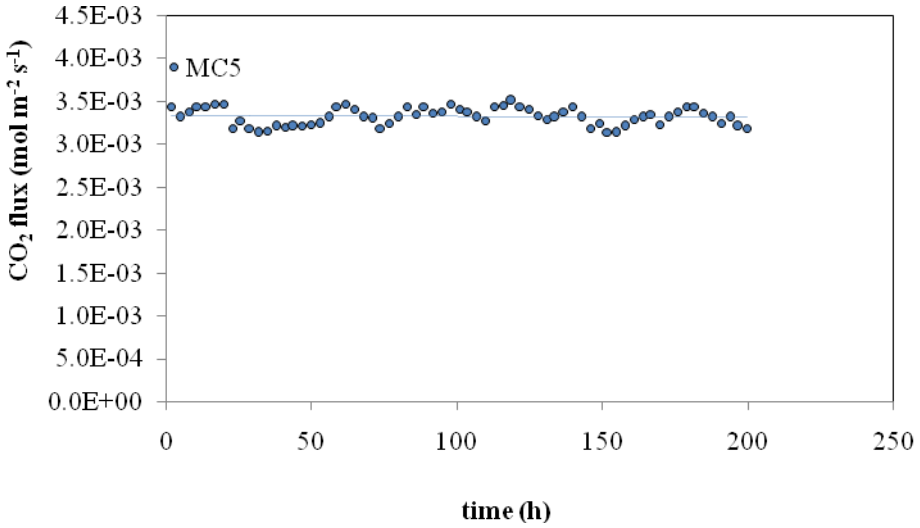

Figure 10. Absorption efficiency of MC5 synthesized membrane in long time (pure CO_2 and nano fluid, T = 25 TC, Pg = 1 × 105 Pa and Pl = 1.2 × 105 Pa

Conclusions

The findings of the present study show that modification of PVDF membranes by combining MWCNT nanotubes results in a better membrane than plain PVDF for use in CO_2absorption when Al_2O_3 is used as a carrier in the absorbent fluid. However, stability studies of membranes fabricated over a period of more than 200 hours using nanofluid absorbents prior to their operation in real commercial applications such as dehumidification and distillation will be very useful. Unlike conventional chemical absorbents such as MEA or DEA, which may facilitate the interaction of PVDF membranes with the absorbent fluid, resulting in the possibility of swelling, structural changes and wetting the membrane pores, the use of absorbent nano fluids in addition In addition to providing high absorption efficiency, it minimizes the mentioned probabilities. Since the absorption flux remained constant during the long process time when using a nanofluid as an absorbent, the negligible effect of the absorbent on the membrane structure could be confirmed, confirming the use of nanofluid absorbents superior to conventional absorbents in gas-liquid contact processes. Performance test of MC5 MMM as a membrane with the best absorption efficiency for9 days and the approximate stability of the efficiency until the end of testing time confirm high tendency of the membrane pores to keep dry.

Acknowledgment

This paper has been extracted from PhD thesis which was done in the Department of Chemical Engineering, Mahshahr branch, Islamic Azad University, Mahshahr, Iran.

References

[1] A. Gabelman, S.-T. Hwang, Hollow fiber membrane contactors, Journal of Membrane Science 159 (1999) 61-106.
[2] J.-L. Li, B.-H. Chen, Review of CO2 absorption using chemical solvents in hollow fiber membrane contactors, Separation and Purification Technology 41 (2005) 109-122.
[3] S.A. Hashemifard, A.F. Ismail, T. Matsuura, M.R. DashtArzhandi, Performance of silicon rubber coated polyetherimide hollow fibers for CO2 removal via a membrane contactor, RSC Advances 5 (2015) 48442-48455.
[4] A.F. Ismail, P.S. Goh, S.M. Sanip, M. Aziz, Transport and separation properties of carbon nanotube-mixed matrix membrane, Separation and Purification Technology 70 (2009) 12-26.

[5] I. Wan Azelee, P.S. Goh, W.J. Lau, A.F. Ismail, M. Rezaei-DashtArzhandi, K.C. Wong, M.N. Subramaniam, Enhanced desalination of polyamide thin film nanocomposite incorporated with acid treated multiwalled carbon nanotube-titania nanotube hybrid, Desalination 409 (2017) 163-170.
[6] S. Lu, Y. Zhao, J. Song, Y. Li, Experimental studies of CO2 absorption enhancement in water-based nanofluids of carbon nanotubes, Brazilian Journal of Chemical Engineering 34 (2017) 597-606.
[7] A. Golkhar, P. Keshavarz, D. Mowla, Investigation of CO2 removal by silica and CNT nanofluids in microporous hollow fiber membrane contactors, Journal of Membrane Science 433 (2013) 17-24.
[8] S. Krishnamurthy, P. Bhattacharya, P.E. Phelan, R.S. Prasher, Enhanced Mass Transport in Nanofluids, Nano Letters 6 (2006) 419-423.
[9] M. Rezaei-DashtArzhandi, A.F. Ismail, G. Bakeri, S.A. Hashemifard, T. Matsuura, Effect of hydrophobic montmorillonite (MMT) on PVDF and PEI hollow fiber membranes in gas-liquid contacting process: a comparative study, RSC Advances 5 (2015) 103811-103821.
[10] M. Rezaei-DashtArzhandi, A.F. Ismail, P.S. Goh, I. Wan Azelee, M. Abbasgholipourghadim, G. Ur Rehman, T. Matsuura, Zeolite ZSM5-Filled PVDF Hollow Fiber Mixed Matrix Membranes for Efficient Carbon Dioxide Removal via Membrane Contactor, Industrial & Engineering Chemistry Research 55 (2016) 12632-12643.
[11] K. Li, Ceramic membranes for separation and reaction, John Wiley & Sons2007.
[12] G. Bakeri, A.F. Ismail, D. Rana, T. Matsuura, M. Shariaty, Investigation on the effects of fabrication parameters on the structure and properties of surface-modified membranes using response surface methodology, Journal of Applied Polymer Science 123 (2012) 2812-2827.
[13] S. Lee, G. Park, G. Amy, S.-K. Hong, S.-H. Moon, D.-H. Lee, J. Cho, Determination of membrane pore size distribution using the fractional rejection of nonionic and charged macromolecules, Journal of Membrane Science 201 (2002) 191-201.
[14] H. Yasuda, J.T. Tsai, Pore size of microporous polymer membranes, Journal of Applied Polymer Science 18 (1974) 805-819.
[15] M. Khayet, C. Feng, K. Khulbe, T. Matsuura, Preparation and characterization of polyvinylidene fluoride hollow fiber membranes for ultrafiltration, Polymer 43 (2002) 3879-3890.
[16] G. Bakeri, A.F. Ismail, M.R. DashtArzhandi, T. Matsuura, Porous PES and PEI hollow fiber membranes in a gas–liquid contacting process—A comparative study, Journal of Membrane Science 475 (2015) 57-64.
[17] A. Mansourizadeh, A.F. Ismail, A developed asymmetric PVDF hollow fiber membrane structure for CO2 absorption, International Journal of Greenhouse Gas Control 5 (2011) 374-380.
[18] G. Bakeri, A.F. Ismail, D. Rana, T. Matsuura, Development of high performance surface modified polyetherimide hollow fiber membrane for gas–liquid contacting processes, Chemical Engineering Journal 198–199 (2012) 327-337.
[19] M. Rezaei, A.F. Ismail, S.A. Hashemifard, G. Bakeri, T. Matsuura, Experimental study on the performance and long-term stability of PVDF/montmorillonite hollow fiber mixed matrix membranes for CO2 separation process, International Journal of Greenhouse Gas Control 26 (2014) 147-157.
[20] M. Rezaei, A.F. Ismail, S.A. Hashemifard, T. Matsuura, Preparation and characterization of PVDF-montmorillonite mixed matrix hollow fiber membrane for gas–liquid contacting process, Chemical Engineering Research and Design 92 (2014) 2449-2460.
[21] M. Rezaei, A.F. Ismail, G. Bakeri, S.A. Hashemifard, T. Matsuura, Effect of general montmorillonite and Cloisite 15A on structural parameters and performance of mixed matrix membranes contactor for CO2 absorption, Chemical Engineering Journal 260 (2015) 875-885.
[22] J.H.J. Kluytmans, B.G.M. van Wachem, B.F.M. Kuster, J.C. Schouten, Mass transfer in sparged and stirred reactors: influence of carbon particles and electrolyte, Chemical Engineering Science 58 (2003) 4719-4728.

[23] R. Wang, H.Y. Zhang, P.H.M. Feron, D.T. Liang, Influence of membrane wetting on CO2 capture in microporous hollow fiber membrane contactors, Separation and Purification Technology 46 (2005) 33-40.
[24] D. Yang, D.J. Devlin, R.S. Barbero, Effect of hollow fiber morphology and compatibility on propane/propylene separation, Journal of Membrane Science 304 (2007) 88-101.
[25] A.M. Barbe, P.A. Hogan, R.A. Johnson, Surface morphology changes during initial usage of hydrophobic, microporous polypropylene membranes, Journal of Membrane Science 172 (2000) 149-156.

HOW TO CITE THIS ARTICLE
Adel Talavari, Bijan Ghanavati, Alireza Azimi, Soheil Sayyahi, PVDF/ MWCNT hollow fiber mixed matrix membranes for gas absorption by Al2O3 nanofluid, Prog. Chem. Biochem. Res. 4(2) (2021) 177-190

DOI: 10.22034/pcbr.2021.270178.1177
URL: http://www.pcbiochemres.com/article_128607.html